Progress In Electromagnetics Research M, Vol. 81, 149–158, 2019

Comparative Study on Sparse and Recovery Algorithms for Antenna Measurement by Compressed Sensing

Liang Zhang[1, 2, *], Tianting Wang[1], Yang Liu[1], Meng Kong[2], and Xianliang Wu[1]

Abstract—Compressed sensing (CS) is utilized in antenna measurements. The antenna data are compressed using the CS method, and the performances of different sparse and recovery algorithms of CS are used to solve antenna measurements. Experiments are conducted on various types of antennas. The results show that efficiency can be greatly improved by reducing the number of measurement points. The best reconstruction performance is exhibited by the Discrete Wavelet Transform (DWT) algorithm combined with the Compressive Sampling Matching Pursuit (COSAMP) algorithm.

1. INTRODUCTION

The traditional sampling theorem is inefficient in many applications because of the large amount of redundant information generated. As a new sensing method, CS has attracted wide attention during recent years in the fields of signal processing and applied mathematics. CS can compress the signals collected on a sensor. The signals can have a sparse or compressible representation in the original or transform domains. This capability is a revolutionary breakthrough that solves the current bottleneck in information acquisition and processing technology. CS has been applied in a large number of fields, such as single-pixel cameras [1], CS-MRI [2], CS Radar [3], wireless sensor networks [4], and SAR imaging [5, 6].

Traditional antenna measurements become more challenging as technology develops. In order to obtain test results quickly and efficiently, the CS method for the far-field region of an antenna measurement system is applied. Migliore introduced the compressed sensing/sparse recovery theory and its usefulness in practical electromagnetic problems [7]. Cornelius et al. exploited the use of relevant information concentrated in a few spherical wave coefficients by reducing the measurement effort and applying them to the theory of spherical near-field to far-field transformation [8]. Another approach reduced the number of measurement points by exploiting the sparsity of the spherical wave spectrum of antennas [9]. The QAIC approach can be used for sparse test results, allowing for efficient and easy antenna measurements [10]. The use of these methods in electromagnetic measurements is relatively new, suggesting the usefulness of the methods in antenna measurements.

To address the shortcomings of traditional sampling theory and signal processing methods, this study explores the recovery performance of antenna far-field signals by using different sparsity bases and reconstruction algorithms. Multiple experiments are conducted on various types of antennas. The results show that the far-field signal can be recovered better under the Discrete Wavelet Transform (DWT) and Compressive Sampling Matching Pursuit (COSAMP) reconstruction algorithms, which improve the measurement efficiency and possess greater advantages and more development potential than traditional antenna measurements.

Received 18 April 2019, Accepted 22 May 2019, Scheduled 10 June 2019

* Corresponding author: Liang Zhang (liangzh@hfnu.edu.cn).

[1] Key Lab of Ministry of Education of Intelligent Computing & Signal Processing, Anhui University, Hefei 230601, China. [2] Anhui Province Key Laboratory of Simulation and Design for Electronic Information System, Hefei Normal University, Hefei 230601, China.

2. COMPRESSED SENSING

The core problems of CS are the sparse transformations and uncorrelated measurements of signals and reconstruction algorithms. The sparseness of a signal can be understood as the number of non-zero elements or absolute value being small. Natural signals are usually not sparse in the real world but can be considered approximately sparse in a certain transform domain. For example, after a natural image is expanded with a two-dimensional wavelet base, most of the expansion coefficients are small, which is the principle that the image can be compressed.

According to the theory of CS [11], the sparsity of the original signal is the premise of the compressed sensing application and determines the number of compressed samples and reconstruction effects. For a signal X of length N, if the signal is sparse or compressible, it can be expressed by Equation (1)

$$X = \sum_{i=1}^{N} \theta_i \Psi_i = \Psi\Theta \tag{1}$$

θ is the coefficient, and Θ is a transform coefficient vector. If the base vector satisfies the orthogonal theorem, then the calculation of the transform coefficient is very easy:

$$\Theta = \Psi^{\mathrm{T}} X \tag{2}$$

The sparse representation of the signal mainly includes a sparse dictionary and a sparse decomposition algorithm. It is important to select an appropriate sparse base for signal processing in order to reduce not only the sampling rate and time but also the data storage and transmission cost.

For a compressible signal, a measurement matrix Φ that is uncorrelated can be constructed to linearly project to the sparse signal. The observation vector is

$$Y = \Phi\Theta = \Phi\Psi^{\mathrm{T}}\mathrm{X} = \mathrm{A}^{\mathrm{CS}} X \tag{3}$$

A^{CS} is a random projection matrix that satisfies the Restricted Isometry Property (RIP). For any K sparse signal X, $\delta_k \in (0, 1)$ satisfies:

$$1 - \delta_k \leq \frac{\|AX\|_2^2}{\|X\|_2^2} \leq 1 + \delta_k \tag{4}$$

The K coefficients can be accurately reconstructed from the M perceptual measurements. In general, the measurement matrix is divided into two categories. The first category consists of random measurement matrices, such as random Gaussian, random Bernoulli, and sparse random matrices. This category has a better recovery effect on the original signal but has strict hardware requirements. The other category consists of deterministic measurement matrices, such as Hadamard, Toeplitz circulant and rotation matrices. Deterministic matrix construction is efficient and easy to implement in hardware.

A signal reconstruction algorithm refers to the process of accurately reconstructing a high-dimensional original signal by the use of low-dimensional data. If the original signal X is sparse, the problem of solving the underdetermined equation $Y = A^{CS}X$ is transformed into the minimum norm problem:

$$\min \left\|\Psi^{\mathrm{T}} X\right\|_0 \text{ s.t } \mathrm{A}^{\mathrm{CS}} X = \Phi\Psi^{T} X = Y \tag{5}$$

This problem is both a non-convex optimization problem and an NP-hard problem that can be replaced by the L_1 norm to transform the problem into a convex optimization problem [12]:

$$\min \left\|\Psi^{\mathrm{T}} X\right\|_1 \text{ s.t } \mathrm{A}^{\mathrm{CS}} X = \Phi\Psi^{T} X = Y \tag{6}$$

The solution to a convex optimization problem has the advantages of stability and uniqueness, as well as being solvable by various optimization methods, such as the interior point, Newton and gradient methods, which are of great significance to signal reconstruction. This paper mainly explores the effects of Compressive Sampling Matching Pursuit (COSAMP) [13], Iterative Reweighted Least Square (IRLS) [14], Greedy Base Pursuit (GBP) [15], Orthogonal Matching Pursuit (OMP) [16], Subspace Pursuit (SP) [17], and Iterative Hard Thresholding (IHT) [18] reconstruction algorithms on the reconstruction far-field data of antennas.

3. EXPERIMENTAL PROCEDURE AND RESULTS

In general, the far-field region of an antenna is sparse or highly compressed in a sparse transform domain Φ, which is usually the DWT, Discrete Cosine Transform (DCT), and Fast Fourier Transformation (FFT). In this study, various types of antennas are verified to explore the effects of different sparse bases and recovery algorithms on the measurement results.

3.1. Standard Gain Pyramid Horn

The sparse performances of pyramid horn antenna far-field data in different transform domains are shown in Fig. 1. The far-field region had the highest sparsity in the DWT domain and the lowest compression ratio in the FFT domain. However, the specific selection of the transform domain is determined by the characteristics of the signal itself. For example, FFT is usually selected in the time domain. The angiography usually selects the equivalent transform because of its sparsity, and DCT is generally used for the compression of the image.

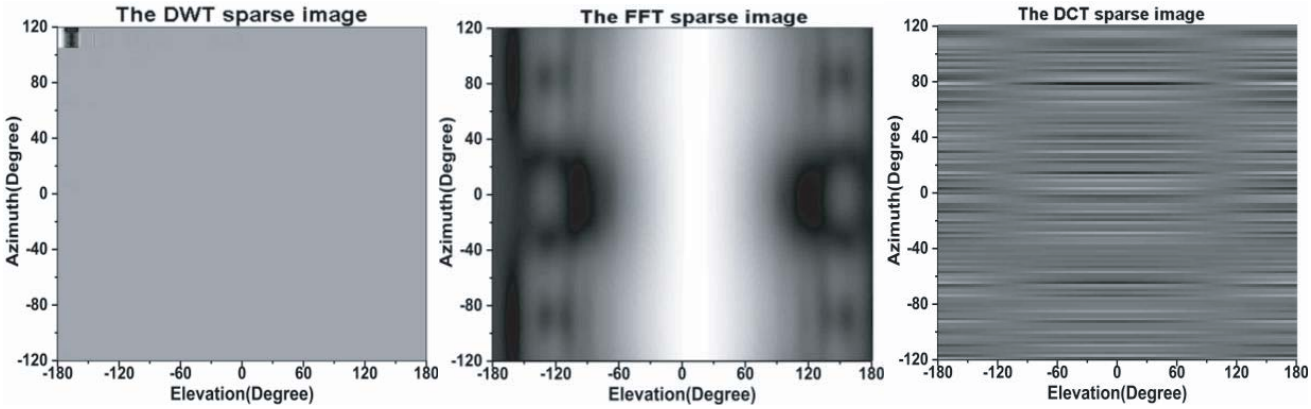

Figure 1. The comparison of far-field of pyramid horn antenna in different transform domains, (a) DWT, (b) FFT, (c) DCT.

The results of the reconstruction using the Gaussian random measurement matrix and OMP reconstruction algorithm with a sparsity ratio of 40% in the far-field region of the pyramidal antenna in different sparse transform domains are shown in Fig. 2. Three kinds of sparse domains are able to recover the original signal. DWT has the best recovery effect, and the E-plane pattern reconstructed signal completely coincides with the original signal, which has better reconstruction accuracy. FFT has the next best effect, and a sharp change error of less than 0.5 is present in the H-plane at -70° but does not affect the recovery of the pattern. DCT has the worst sparse domain with large errors at multiple angles. The pattern recovery contains a disturbance, but the antenna far-field is basically recovered.

The traditional antenna measurement method is about 360 seconds, which requires 1800 measurement points (in a 360° range) for the experimental pyramid antenna. Table 1 shows the recovery error, time consumption, signal to noise ratio (SNR), and signal distortion rate (SDR) of the three methods when the sampling rate M/N is 0.2, 0.3, and 0.4 in different sparse bases. The signal distortion rate (SDR) is:

$$\mathrm{SDR} = 10\log 10\left(\frac{\sum_{N=0}^{N-1}\left\|y_{\mathrm{Original}}\right\|_2}{\sum_{N=0}^{N-1}\left\|y_{\mathrm{Original}} - y_{\mathrm{Recovery}}\right\|_2}\right) \tag{7}$$

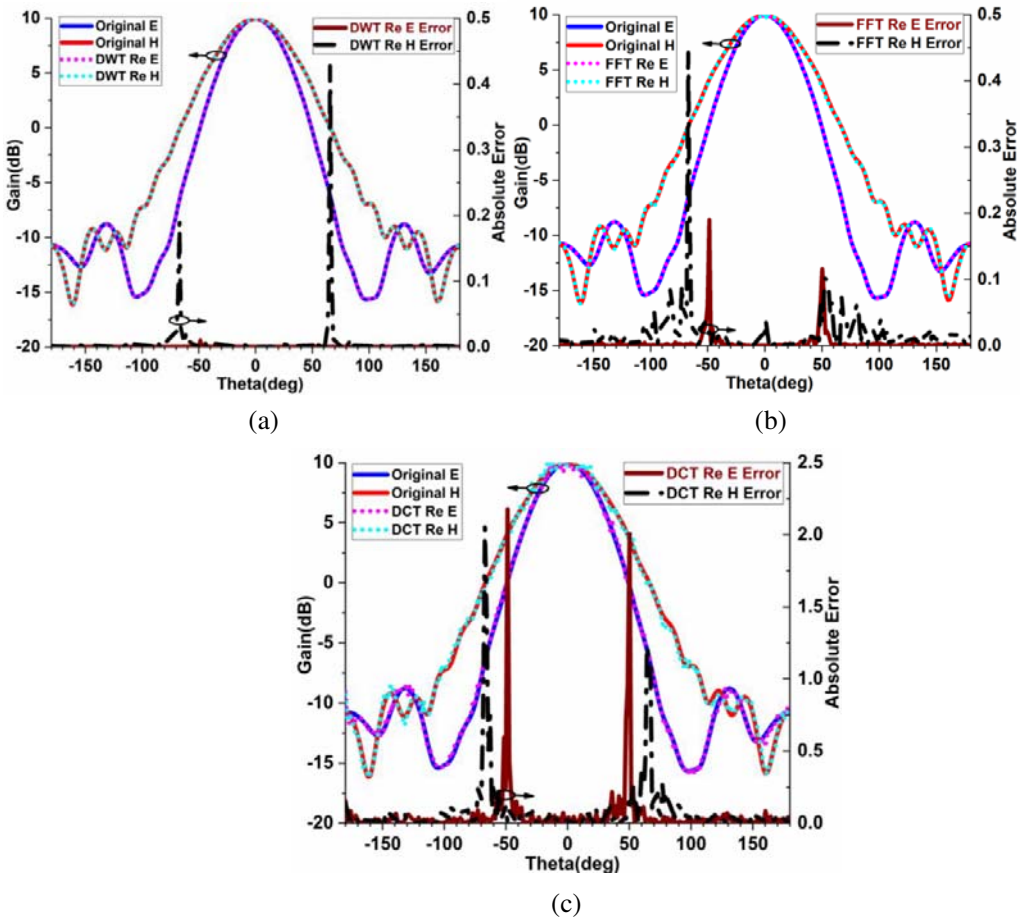

Figure 2. Reconstruction effect of the pyramid antenna far-field in different sparse domains, (a) DWT, (b) FFT, (c) DCT.

Table 1 shows that as the sampling rate increases, the reconstruction error significantly decreases, and the antenna far-field region can be accurately reconstructed at a low sampling rate. The measurement time is proportional to the sparse ratio, and the DWT sparse domain has the highest operating efficiency. When the compression ratio is 0.4, the original signal can be recovered better. The measurement time is 155 seconds, which is a 57% improvement compared to the traditional measurement.

From the above results, we can know that the antenna far-field can be reconstructed almost perfectly with the OMP recovery algorithm. However, for specific sparse domains and measurement matrices, different recovery algorithms may exhibit different efficiencies and accuracies. Therefore, it is especially important to explore the recovery algorithm for antenna far-field reconstruction. The antenna far-field region is sparseness by DWT, and the Gaussian random matrix is selected as the CS measurement matrix. The recovery performances under different recovery algorithms at a sparse ratio of 0.4 are depicted in Fig. 3.

Fig. 3 shows that OMP, COSAMP, and IRLS have better reconstruction effects, and the original signal has been reconstructed without error. The COSAMP performance is optimal, and the reconstruction is stable and accurate. The SP recovery effect is slightly deviated; the accuracy is low; and the general trend of the far-field map can be recovered, but the original signal cannot be recovered. The recovery effects of GBP and IHT are extremely poor, and the original signal cannot be recovered. The GBP recovery signal value has a large error. IHT can recover the far-field pattern but cannot restore the amplitude very well. The two recovery algorithms should not be used as antenna far-field recovery algorithms.

Table 1. Comparison of performance of far-field in different sparse bases.

	Sparse Ratio (%)	Recovery Error (dB)	Recovery Times (s)	SNR (dB)	SDR
FFT	20	0.34	80	9.37	4.68
	30	0.21	123	13.56	6.78
	40	0.08	202	21.94	10.97
DCT	20	0.46	82	6.74	3.37
	30	0.33	119	9.63	4.81
	40	0.11	186	18.17	9.59
DWT	20	0.31	75	10.17	5.09
	30	0.18	102	14.89	7.45
	40	0.009	155	40.92	20.46

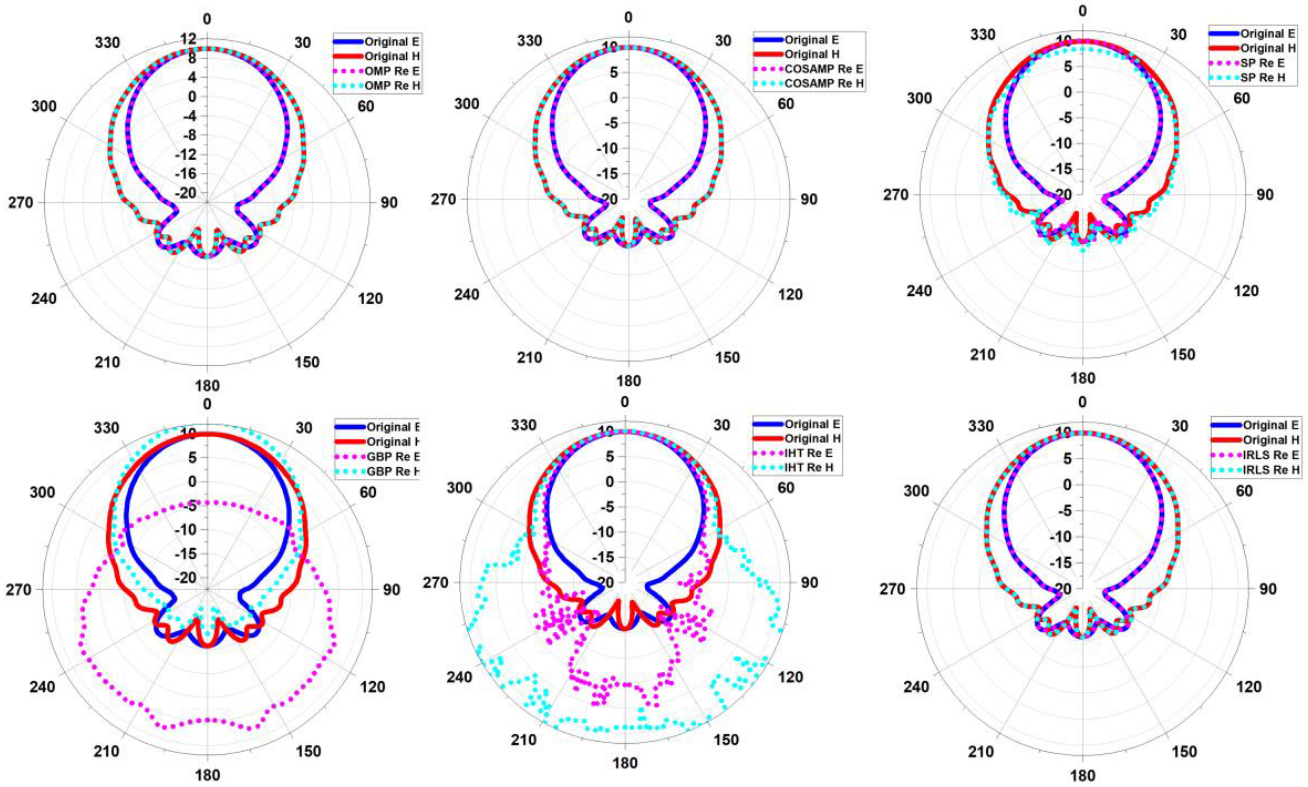

Figure 3. Reconstruction of the antenna far-field in different recovery algorithms.

3.2. Array Antenna

The sparse performance for an array antenna is similar to that of the pyramid horn antenna, as shown in Fig. 4. It is advantageous for far-field data using wavelet sparse. A comparison of the sparseness of the three sparse bases shows that the DCT exhibits a sparse performance worse than those of the other algorithms for antenna far-field measurement.

The results of the reconstructed signal with a sparsity ratio of 40% in the far-field region of the array antenna in different sparse transform domains are shown in Fig. 5. DWT has the best recovery effect, by which the E-plane and H-plane patterns are reconstructed perfectly. There is a sharp change

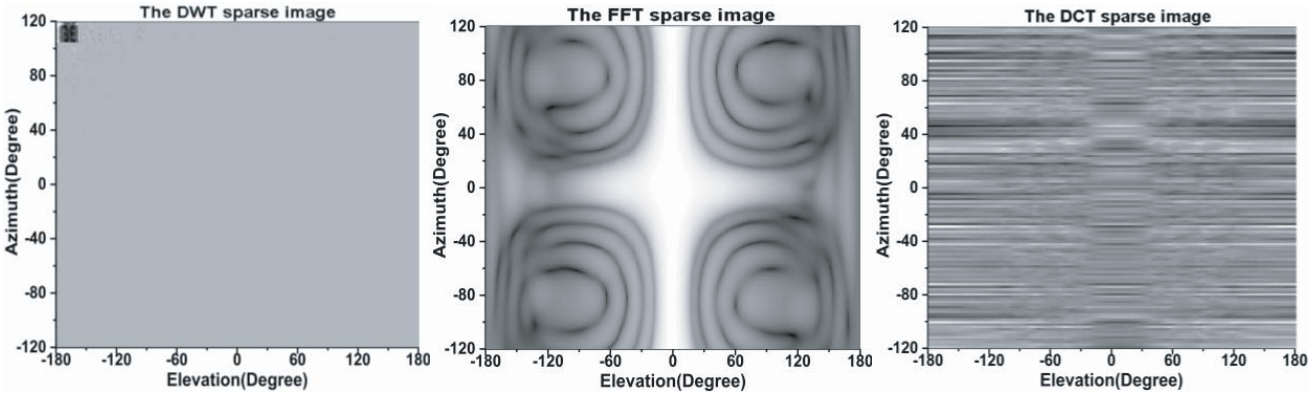

Figure 4. The comparison of far-field of an array antenna in different transform.

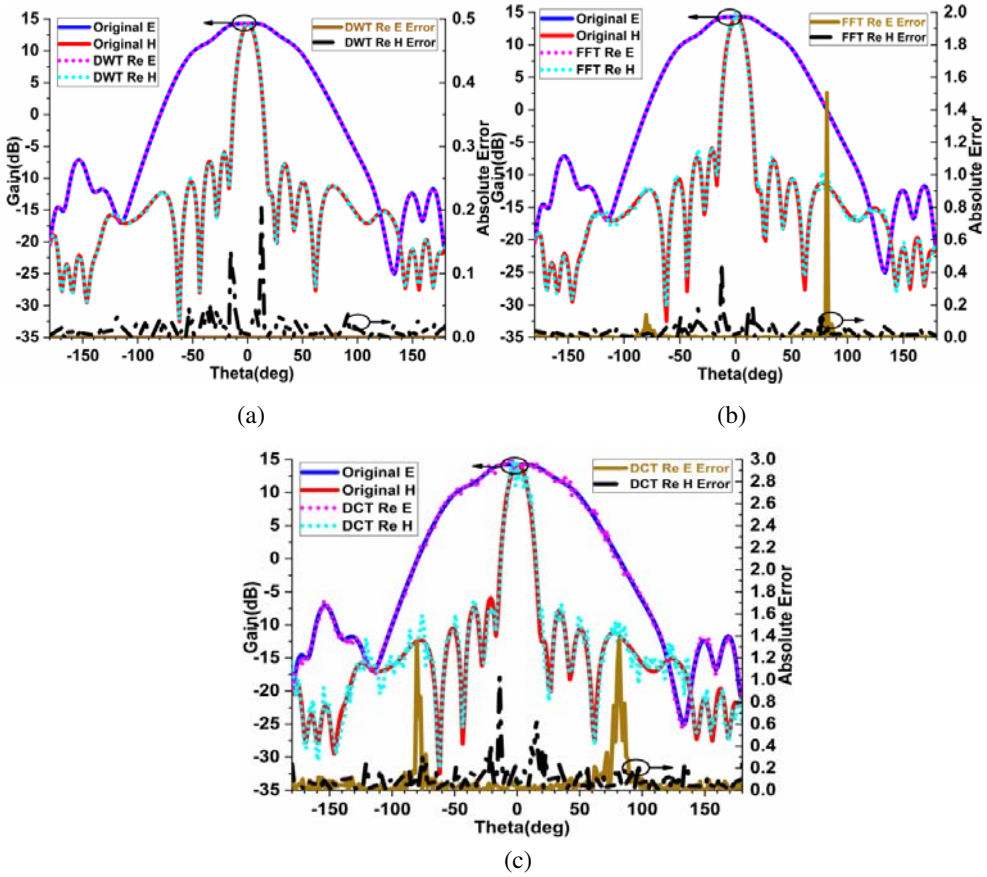

Figure 5. Reconstruction effect of the array antenna far-field in different sparse domains, (a) DWT, (b) FFT, (c) DCT.

error of 1.58 in the E-plane at 85°. Some deviations from the H-plane recovery may be the more side beam for FFT. It has a worse performance for reconstruction and is unable to recover the original signal for DCT. There are also large errors at different angles.

The traditional far-field pattern that is measured requires 5400 points (360° range), and the entire measurement time is 540 seconds, which is longer. Table 2 shows that when the sparse ratio is 0.4,

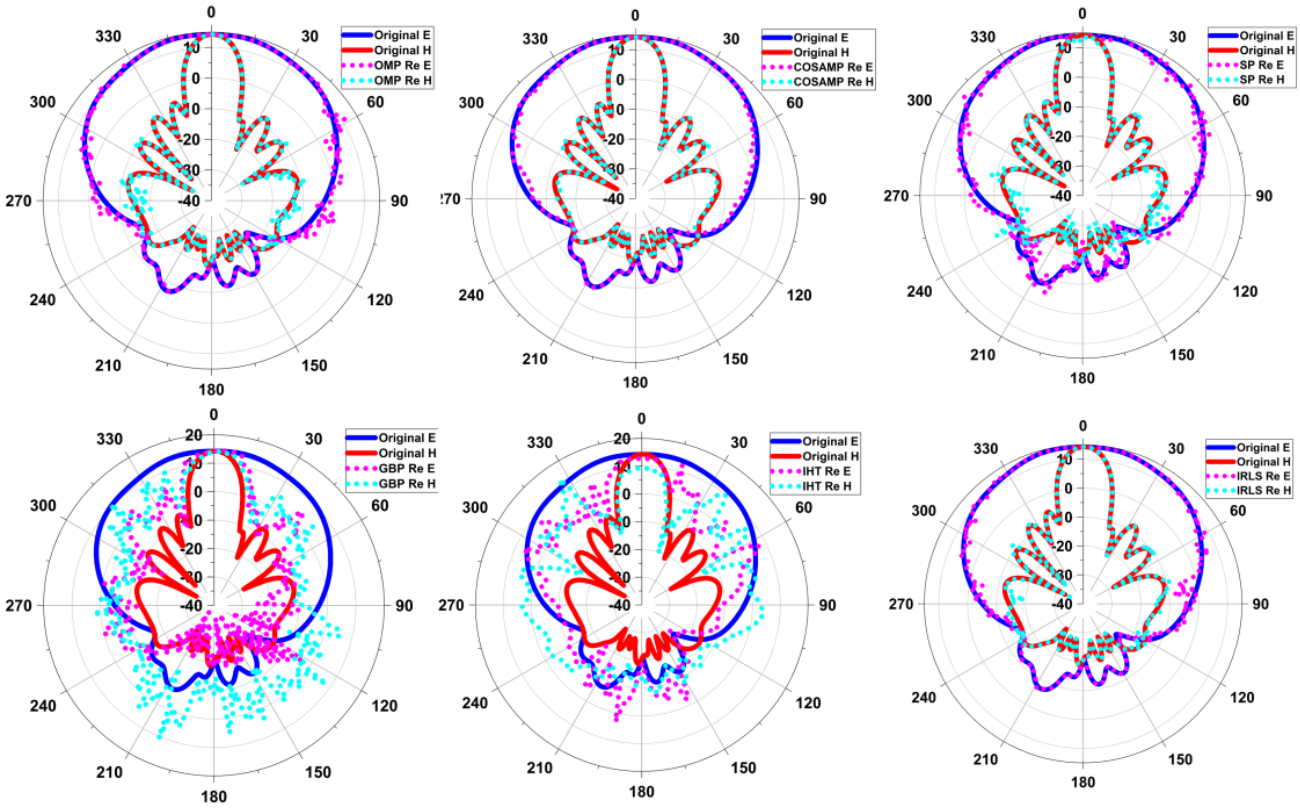

Figure 6. Reconstruction of an array antenna far-field in different recovery algorithms.

DWT has better recovery performance. The optimal measurement time is 212 seconds, which is a 61% improvement compared with the traditional measurement time.

The antenna far-field recovery performances of different recovery algorithms are shown in Fig. 6. It is clear that COSAMP has the best reconstruction performance of all the algorithms we used. OMP, IRLS, and SP are not as good as COSAMP for reconstruction. However, the approximate outline of the antenna far-field region could be restored. GBP and IHT have the worst recovery effects and cannot be used as antenna far-field recovery algorithms.

Table 2. Comparison of performance of far-field in different sparse bases.

	Sparse Ratio (%)	Recovery Error (dB)	Recovery Times (s)	SNR (dB)	SDR
FFT	20	0.35	135	9.12	4.56
	30	0.23	201	12.77	6.38
	40	0.006	243	44.43	22.21
DCT	20	0.51	138	5.85	2.92
	30	0.38	192	8.41	4.21
	40	0.13	246	17.70	8.86
DWT	20	0.42	112	7.54	3.77
	30	0.15	171	16.47	8.24
	40	0.004	212	48.01	23.8

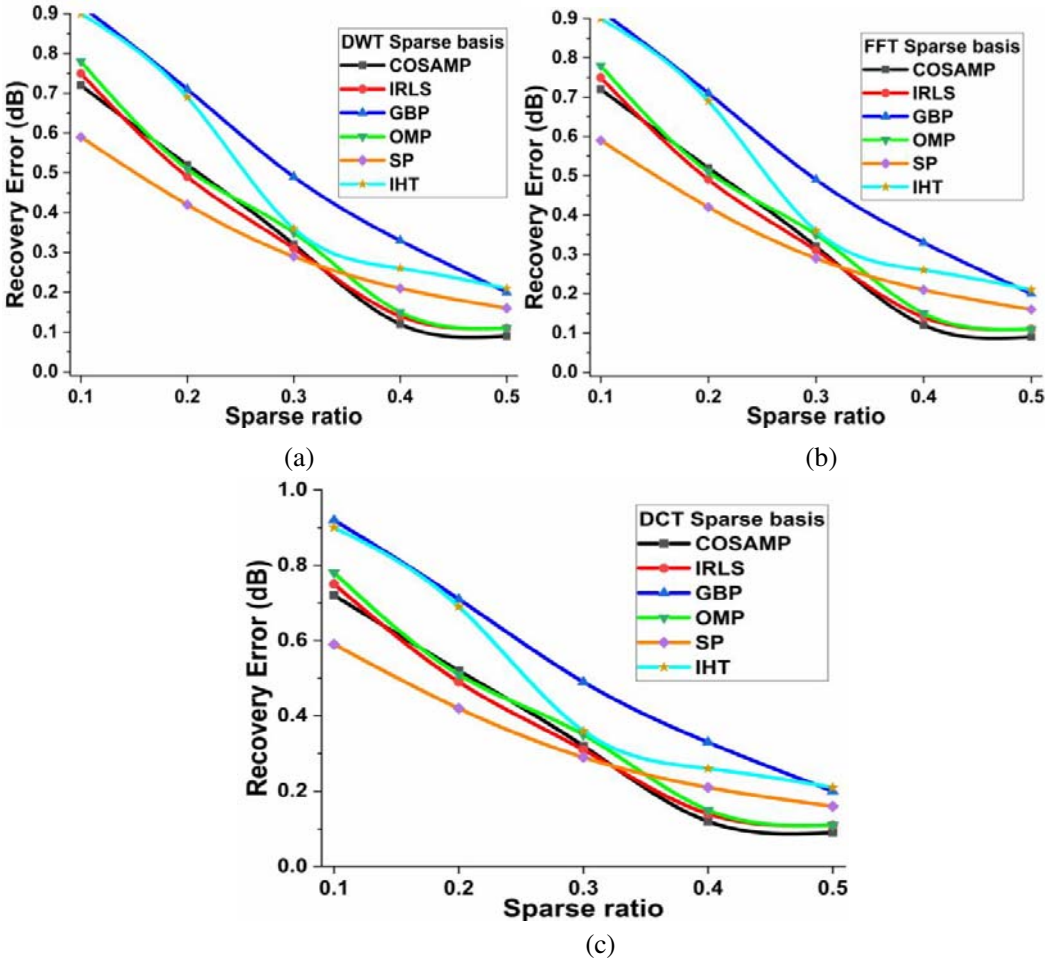

Figure 7. The average error of multiple sparsity bases and recovery algorithms with various antennas measurement in different sparse ratios, (a) DWT, (b) FFT, (c) DCT.

Table 3. Comparison of reconstruction effects of different recovery algorithms.

ALGORITHMS	Index	Index update	Update iteration	Stability	Accuracy
COSAMP	$u = \langle r_{r-1}, a_j \rangle, 1 \le j \le N$ $J = \{2Kl \arg estu\}$	$\Lambda_t = \Lambda_{t-1} \cup J_0$ $A_t = A_{t-1} \cup a_j$	$t > k$ or $r_t = 0$	yes	superior
IRLS	$\theta = \Omega^T \ y \ p = 1, \varepsilon = 1$	$\theta = Q\Omega^T inv\left(\Omega Q \Omega^T\right)$	$w_i = \left(\theta_i^2 + \varepsilon\right)^{p/2-1}$	no	well
GBP	$I = \emptyset, \theta = O \in R^m$	$i = \arg\max_j \lvert\langle \omega_j, n \rangle\rvert$ $I = \{i\}$	$d_H = \langle \omega_I, n \rangle$ $y_H = \left(\frac{d_H}{\langle y_H, n \rangle}\right) y$	no	bad
OMP	$\lambda_t = \arg \max_{j=1,2,\cdots d} \lvert\langle r_{t-1}, \Phi \rangle\rvert$	$\Lambda_t = \Lambda_{t-1} \cup \lambda_t$	$t = k$	yes	well
SP	$u = \langle r_{t-1}, a_j \rangle, 1 \le j \le N$ $J = \{Kl \arg estu\}$	$\Lambda_t = \Lambda_{t-1} \cup J_0$ $A_t = A_{t-1} \cup a_j$	$y_r = 0$ or $y_r = \hat{y}_r$	yes	low
IHT	$k = \left[\log_2 \frac{\lVert y^s \rVert_2}{\lVert e \rVert_2}\right]$	$\Gamma^* = \sup p\{y^s\}$ $\Gamma^n = \sup p\left\{y^{[n]}\right\}$	$B^{n+1} = \Gamma^* \cup \Gamma^{n+1}$	no	bad

4. RECOVERY PERFORMANCE OF CS FOR ANTENNA MEASUREMENTS

In order to demonstrate that the experiments are not only effective for special antennas, various types (more than a dozen) of antennas are also verified (more than 30 times) to explore the effects of different sparsity bases and recovery algorithms on antenna measurement. Fig. 7 shows the average errors of multiple sparse bases and different recovery algorithms with multiple antenna measurements at different sparse ratios.

Figure 7 shows that as the sparse ratio increases, the reconstruction error gradually decreases, and the reconstruction effects of the three sparse domains are roughly similar. When the sparseness is low, the SP recovery algorithm is better, but there is a large reconstruction error, and the signal cannot be recovered well. The recovery performance of the GBP is the worst in the DCT sparse domain when the sparse ratio is 0.1, and the maximum error is 0.92. When the sparse ratio is more than 0.4, the recovery errors of the COSAMP and OMP algorithms tend to be stable. The original signal can be recovered well with an error of less than 0.1. The reconstruction errors of COSAMP and OMP in DWT are 0.006 and 0.007, respectively. The recovery of the original signal is better. The mechanisms and recovery performances of various recovery algorithms are shown in Table 3.

5. CONCLUSION

This study focuses on the development of antenna measurement and compressed sensing. Experiments are conducted on various antennas. The far-field region of each antenna is reconstructed by different sparse domains and recovery algorithms, whose performances are compared and analyzed. The combination of the DWT and COSAMP reconstruction algorithms is able to recover the signal better in the far-field region, as well as improve the efficiency and greatly reduce the time of antenna measurement.

ACKNOWLEDGMENT

This research was partially supported by Major Project of Provincial Natural Science Research of University of Anhui Province of China (Grant No. KJ2018ZD046 and No. 2017sxzx40), and the National Natural Science Foundation of China (Grant No. 61801163 and No. 61871001).

REFERENCES

1. Duarte, M. F., et al., "Single-pixel imaging via compressive sampling," *IEEE Signal Processing Mag.*, Vol. 25, No. 2, 83–91, 2008.
2. Lustig, M., D. Donoho, and J. M. Pauly, "Sparse MRI: The application of compressed sensing for rapid MR imaging," *Magnetic Resonance in Medicine*, Vol. 58, No. 6, 1182–1195, 2007.
3. Paredes, J. L., G. R. Arce, and Z. Wang, "Ultra-wideband compressed sensing: Channel estimation," *IEEE Journal of Selected Topics in Signal Processing*, Vol. 1, No. 3, 383–395, 2007.
4. Bajwa, W., et al., "Compressive wireless sensing," *International Conference on Information Processing in Sensor Networks ACM*, Vol. 402, No. 2, 134–142, 2006.
5. Chang, J., W. Zhang, S. Zhang, et al., "A novel SAR imaging algorithm based on compressed sensing," *IEEE Cie International Conference on Radar, IEEE*, 2006.
6. Lin, X. H., G. Y. Xue, and P. Liu, "Novel data acquisition method for interference suppression in dual-channel SAR," *Progress In Electromagnetics Research*, Vol. 144, 79–92, 2014.
7. Migliore, D. M., "A simple introduction to compressed sensing/sparse recovery with applications in antenna measurements," *IEEE Antennas and Propagation Magazine*, Vol. 56, No. 2, 14–26, 2014.
8. Cornelius, R., D. Heberling, N. Koep, et al., "Compressed sensing applied to spherical near-field to far-field transformation," *European Conference on Antennas and Propagation, IEEE*, 2016.
9. Fuchs, B., L. L. Coq, S. Rondineau, et al., "Fast antenna far-field characterization via sparse spherical harmonic expansion," *IEEE Transactions on Antennas & Propagation*, Vol. 65, No. 99, 1–1, 2017.

10. Zhang, L., F. Wang, T. Wang, X. Y. Cao, M. S. Chen, and X. L. Wu, "Fast antenna far-field measurement for sparse sampling technology," *Progress In Electromagnetics Research M*, Vol. 72, 145–152, 2018.
11. Donoho, D. L., "Compressed sensing," *IEEE Transactions on Information Theory*, Vol. 52, No. 4, 1289–1306, 2006.
12. Donoho, D. L., Y. Tsaig, I. Drori, et al., "Sparse solution of underdetermined systems of linear equations by stagewise orthogonal matching pursuit," *IEEE Transactions on Information Theory*, Vol. 58, No. 2, 1094–1121, 2012.
13. Needell, D. and J. A. Tropp, "CoSaMP: Iterative signal recovery from incomplete and inaccurate samples," *Appl. Comput. Harmon. Anal.*, Vol. 26, No. 3, 301–321, 2008.
14. Chartrand, R. and W. Yin, "Iteratively reweighted algorithms for compressive sensing," *IEEE International Conference on Acoustics, Speech and Signal Processing, 2008, ICASSP 2008, IEEE*, 2008.
15. Huggins, P. S. and S. W. Zucker, "Greedy base pursuit," *IEEE Transactions on Signal Processing*, Vol. 55, No. 7, 3760–3772, 2007.
16. Tropp, J. A. and A. C. Gilbert, "Signal recovery from random measurements via orthogonal matching pursuit," *IEEE Transactions on Information Theory*, Vol. 53, No. 12, 4655–4666, 2007.
17. Dai, W. and O. Milenkovic, "Subspace pursuit for compressive sensing signal reconstruction," *IEEE Transactions on Information Theory*, Vol. 55, No. 5, 2230–2249, 2008.
18. Blumensath, T. and M. E. Davies, "Iterative hard thresholding for compressed sensing," *Applied & Computational Harmonic Analysis*, Vol. 27, No. 3, 265–274, 2008.